Energy scaling of Kerr-lens mode-locked thin-disk oscillators

Jonathan Brons,[1,*] Vladimir Pervak,[2] Elena Fedulova,[1] Dominik Bauer,[3] Dirk Sutter,[3] Vladimir Kalashnikov,[4] Alexander Apolonskiy,[1,2] Oleg Pronin,[2] and Ferenc Krausz[1,2]

[1]*Max-Planck-Institut für Quantenoptik, Garching, Germany*

[2]*Ludwig-Maximilians-Universität München, Garching, Germany*

[3]*TRUMPF Laser GmbH, Schramberg, Germany*

[4]*Institut für Photonik, TU Wien, Vienna, Austria*

**Corresponding author: jonathan.brons@mpq.mpg.de*

Received August 7, 2014; revised September 30, 2014; accepted October 2, 2014; posted October 9, 2014 (Doc. ID 220568); published November 10, 2014

Geometric scaling of a Kerr-lens mode-locked Yb:YAG thin-disk oscillator yields femtosecond pulses with an average output power of 270 W. The scaled system delivers femtosecond (210–330 fs) pulses with a peak power of 38 MW. These values of average and peak power surpass the performance of any previously reported femtosecond laser oscillator operated in atmospheric air. © 2014 Optical Society of America

OCIS codes: (140.4050) Mode-locked lasers; (140.7090) Ultrafast lasers; (140.3580) Lasers, solid-state; (140.3480) Lasers, diode-pumped.

http://dx.doi.org/10.1364/OL.39.006442

Over the last two decades, the average output power and pulse energy from ultrafast lasers have grown remarkably, paving the way toward new scientific and technological applications. Average power and energy scaling has been demonstrated with multipass MHz amplifiers [1–3] as well as directly with oscillators [4–7], with the latter offering lower noise, lower cost, and simpler, more user-friendly setup. Moreover, in several applications such as cold target recoil ion momentum spectroscopy (COLTRIMS), time-resolved photoemission electron microscopy (PEEM) and femtosecond electron diffraction, the output from high-power MHz-repetition-rate oscillators can drastically improve the signal-to-noise ratio, reducing both measurement time and uncertainties [8].

The diode-laser-pumped thin-disk (TD) technology [9] has proven particularly powerful in scaling femtosecond oscillators to unprecedented peak and average power levels. Yb:YAG TD oscillators mode-locked with a semiconductor saturable absorber mirror (SESAM) are now approaching the peak power level of 100 MW when operated in vacuum or inert-gas atmosphere [5–7]. This is needed to avoid nonlinear phase shifts accumulated in atmospheric air, which would typically destabilize mode-locking by a SESAM due to its small modulation depth and slow response time [10] as compared to Kerr-lens mode-locking (KLM) [11,12]. In the absence of atmospheric air, such oscillators have recently yielded average powers as high as 275 W and pulse energies of 80 μJ with pulse durations around 1 ps [5,6].

By contrast, Kerr-lens mode-locking offers near-gain-bandwidth-limited pulses [13,14] and since its first demonstration in a TD oscillator [15] KLM oscillators have proven an excellent power and energy scalability (see red stars in Fig. 1—original data and references in [4–7,16–24]). By implementing geometric scaling of a KLM TD oscillator, the performance of the first demonstrator [15] could be surpassed by a factor of 10 in pulse energy and 6 times in average power. Thanks to the dominance of the contribution of the Kerr medium (KM) to the total nonlinear phase-shift, the operation of the system is largely unaffected by a change of atmosphere. This scaled femtosecond KLM oscillator can therefore be reliably operated in atmospheric air, attaining, under these conditions, unprecedented peak and average power.

In traditional KLM oscillators, both KLM and light amplification is provided by the laser crystal with its circular gain volume forming the (soft) aperture for KLM [25–27]. Separation of gain and Kerr-nonlinearity offers several advantages. First, the Kerr lensing effect can be optimized independently of the round-trip gain by suitable choice of the material, thickness and position of the Kerr medium (KM) and the mode size in the KM. Second, it is easier to position the TD such that the soft-aperture effect optimizes self-amplitude modulation (SAM) [25,28] and thereby the peak power of the circulating femtosecond pulse.

This optimization requires a careful balance between maximization and saturation of SAM. Saturation can be understood by inspecting the overlap of the fundamental cavity mode with the pumped area. Starting from an oversized mode, the overlap (and therefore gain) increases with the laser mode shrinking, until it reaches an

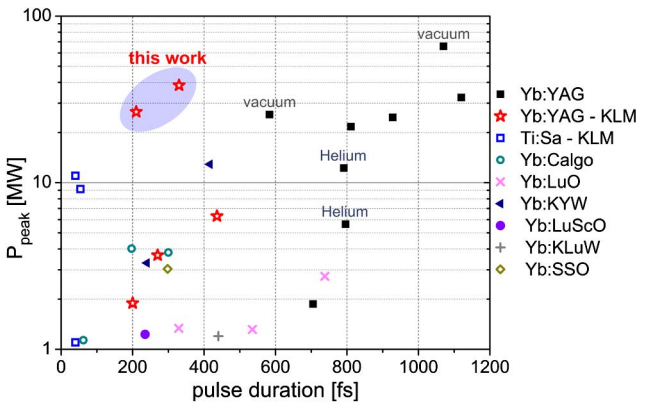

Fig. 1. Comparison of output peak-power from high-power mode-locked oscillators. All are mode locked by a SESAM, except those marked KLM.

optimum. Reducing the mode size further starts decreasing the (saturated) round-trip gain (obviously one can also begin with a small mode and then improve the overlap by expanding the beam). By choosing the right boundary of the resonator's stability region [29–31] as well as optimizing the distances of the TD and the hard-aperture from the KM, we were able to maximize the spectral width and output-power.

Since the average mode-size scales with the resonator length, one can hardly reach simultaneously a high pulse repetition rate and a large mode in the gain-medium. This will set a limitation to the available roundtrip gain in the oscillator as the pump-intensity on the TD cannot be increased arbitrarily but has to be accompanied by a proportional growth of the pumped area as well as the mode area. In this experiment no restrictions had been imposed on the repetition rate such that the only requirement on the oscillator mode was to overlap with the pumped region for optimum laser efficiency. In this case, a simple cavity of z-shape type could be chosen without additional beam-expanding elements. The nearly flat, 120-μm-thin Yb:YAG disk (TRUMPF GmbH) is placed between a plane output coupler and a plane end-mirror. It is sufficiently wedged to separate residual reflections off the AR-coated front facet from the main beam. The optical beam path is folded for two reflections on the TD in one direction, resulting in 4 reflections on the disk per roundtrip [see Fig. 2 (left)]. The 8-fold passage of the mode through the disk boosts the round-trip gain and allows for high output-coupling ratios while increasing the optical-to-optical efficiency [4,22]. For all presented experiments hereafter, an output coupler with 21% transmission was used. Fundamental TEM_{00} mode selection was accomplished by scaling the $1/e^2$ Gaussian mode-diameter to approx. 70% of the pump-spot with ~3.5 mm diameter. By introducing a focusing section, consisting of two focusing mirrors, FM1 and FM2 [Fig. 2 (left)], a small focal spot is set in the 1-mm-thick sapphire KM, providing the necessary SAM for starting mode locking and spectral broadening via self-phase modulation (SPM). This focusing section was chosen to be symmetric to avoid a change in the beam size or phase-front curvature elsewhere in the resonator.

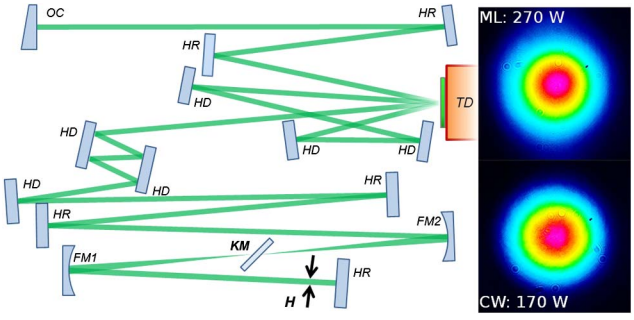

Fig. 2. (left) Resonator sketch (not to scale). OC, out-coupler; HR, high reflective mirror; HD, high dispersive mirror; TD, thin-disk (19-m radius of curvature); FM1/FM2, focusing mirrors 1&2; KM, Kerr-medium; H, aperture with 5-mm diameter. (right) The low power 170 W CW and high power 270 W ML beam profiles are depicted. The similarity of the beam profiles is due to the spatial filtering of the hard aperture, cutting off the strongly astigmatic parts of the CW mode in the tangential plane approx. 1 m away from OC.

For initiating KLM, strong sensitivity of the resonator mode to the Kerr lens is required. This sensitivity is maximized at the boundaries of a resonator's stability zone [32]. To this end, the separation between mirrors FM1 and FM2 is slightly changed from the neutral imaging configuration, shifting the resonator to the edge of its stability zone. After doing so, the free-running oscillator can be mode-locked by perturbing one of the focusing mirrors and with proper positioning of the KM even self-starting operation is possible. The resulting Kerr-lens then shifts the resonator back toward the stability center. In such a cavity configuration, mode locking is possible by only exploiting the soft aperture of the pumped region. The pulse buildup induced by the soft aperture only is found to frequently result in the onset of chaotic, Q-switching-like intensity fluctuations, which may lead to damage of the cavity optics. In the first KLM TD oscillator, this problem was mitigated by the introduction of a weak SESAM covered by a dielectric coating [15]. In this work, the SESAM was replaced with a hard aperture formed by a water-cooled copper plate with a drilled hole.

Mode-locked operation in the regime of anomalous dispersion is realized by up to 8 bounces on high-dispersive folding mirrors [33] introducing a total round-trip group delay dispersion (GDD) of $-48,000$ fs^2. The soliton area theorem [34–36] predicts the pulse energy E of a soliton to be $E \propto (P_{\mathrm{th}}|\beta|/\gamma)^{1/2}$ (P_{th}: maximal threshold peak power for stable soliton; β: group delay dispersion; γ: coefficient of self-phase modulation). However, the area theorem is not sufficient per se for an explanation of the soliton energy scalability, because the threshold peak power P_{th} is defined by many factors (modulation depth, dissipation, and amplification) tied to a specific laser-oscillator setup. An energy scaling law can be derived by a variational approximation of the nonlinear complex Ginzburg–Landau model of laser solitons [37,38]. A detailed theoretical analysis of this problem is in preparation [39].

The nonlinear phase shift can be controlled by changing the thickness of the gain medium, the KM, and the atmospheric conditions and/or by altering the mode-size. In our relatively short resonator (>10 MHz), the contribution of the atmosphere can be neglected, and in this case of short focal lengths (≤1 m), SPM happens mainly in the KM. With increasing Rayleigh length of the focus between FM1 and FM2, the contribution of air to the total nonlinear phase-shift grows. A certain thickness of the KM is needed to provide sufficient SAM for pulse stabilization and just as importantly, initiation of KLM. Moreover, the additional spectral broadening via SPM often is a desired effect for obtaining shorter pulses [40,41]. A changed geometry will affect various other parameters of the oscillator as well, among them the SAM modulation depth and its saturation, which are not described by the area theorem. Introducing more GDD will not raise the peak power as the pulse duration will increase along with the pulse energy [34,35,37] (see blue curve in Fig. 3).

The results reported on here were obtained following an easy-to-implement scaling procedure based purely on

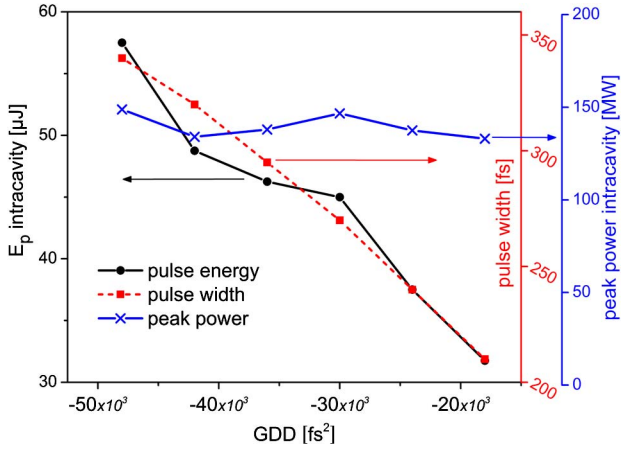

Fig. 3. Intracavity peak power, pulse energy and width for the GDD range $-48,000 - 18,000$ fs^2. The peak power stays approximately constant as the pulse duration decreases. The hard aperture for these measurements had a diameter of 5.5 mm.

geometrical considerations. This energy scaling scheme is made possible by decoupling the Kerr lensing from the light amplification and is described below.

Let us consider the resonator sketched in Fig. 2 for an increasing cavity mode size w_k in the KM by a scaling factor N. This factor can be controlled by the radius of curvature of the focusing mirrors FM1 and FM2 [Fig. 2 (left)]. With all other resonator parameters fixed, the maximum achievable peak power is then expected to scale with N^2 (for a certain value of the maximum intensity in the KM). This is equivalent to rescaling the SPM coefficient γ. The pulse energy in this simplified picture scales with the mode-area, N^2, in the KM. However, also taking into account the dependence of dissipative factors in the variational approximations, a detailed analysis yields the linear relation $E \propto N$ [39].

In Fig. 4 the described dependence is demonstrated by a fit of the linear scaling law to measured values of the intracavity pulse energy versus different mode sizes in the KM. This parameter was varied by changing the radii of curvature (ROC) of the focusing mirrors FM1 and FM2

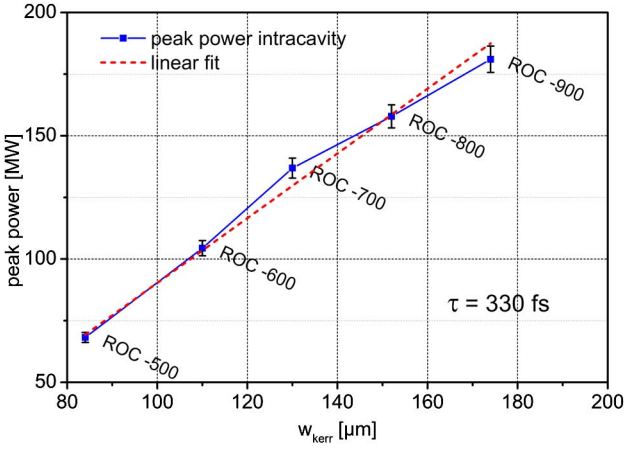

Fig. 4. Intracavity pulse energies for different ROC of FM1 & FM2. The mode size w_{Kerr} in the KM is estimated with the ray transfer matrix formalism in CW limit at the stability center. In reality, w_{Kerr} may differ. The pulse duration for all parameter sets remained constant at Fourier-limited 330 fs.

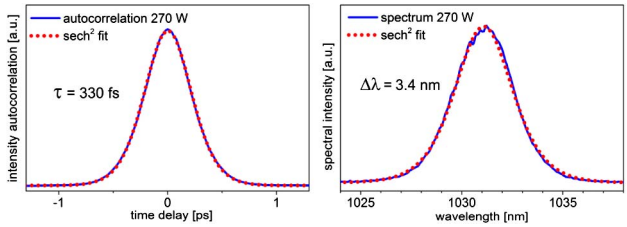

Fig. 5. Intensity autocorrelation trace (left) and spectral intensity (right) proving Fourier-limited (time-bandwidth product: 0.32) pulses for –900 mm ROC focusing mirrors, 270-W average output power at 330-fs pulse-duration with 3.4-nm spectral width (FWHM).

from –500 to –900 mm. Ray-transfer matrix simulations reflect the proportional increase in mode radius w_k, although real values might differ. All other parameters, such as the GDD, stayed constant. Figure 4 reveals linear increase in pulse energy with the mode size at a constant Fourier-limited pulse duration of 330 fs, in accordance with the above geometrical scaling considerations. With the ROC of –900 mm and the roundtrip GDD of –48000 fs^2, an average output-power of 270 W could be measured, corresponding to 14.4 µJ pulse energy at 18.8 MHz repetition rate. The intensity autocorrelation and mode-locked spectrum shown in Fig. 5 indicate Fourier-limited 330-fs sech^2 pulses, implying pulses with a peak power of 38 MW. The optical-to-optical efficiency at this power level is 36% with a beam quality factor M^2 better than 1.1. The RMS intensity fluctuation is measured as 1% over the bandwidth of 1 Hz–1 MHz. Systematically reducing the GDD from $-48,000$ fs^2 to $-18,000$ fs^2 yielded 230-W, 340-fs reducing to 127-W, 210-fs pulses (see Fig. 3, for these measurements the hard aperture diameter was 5.5 mm). While the pulse energy decreases for lower values of the GDD the peak power remains constant, underpinning the scaling behavior predicted by the area theorem.

Technical challenges toward higher average powers are imposed by the thermal load on intracavity optics. The difference between 1.3 kW average intracavity power in ML and 0.8 kW in CW operation causes different thermal lenses in the TD and also the intracavity optics, effectively shifting and expanding the zone of stability [42,43]. This can move the working point of the resonator into the stable zone, reducing the modulation depth and the sensitivity to the Kerr-lens, which results in a narrower spectrum, longer pulses, and lower pulse energy. These cumulative lensing effects can be counteracted partially by adjusting the separation distance of mirrors FM1 and FM2. In this work the thermal effects were reduced mainly by the following measures: one was replacing the fused silica KM [15] with sapphire. The thermal design of the intracavity optics, especially high dispersive mirrors, is also likely to play a role in KLM performance [44]. Thus the multilayer design and coating of the HD mirrors were optimized to exhibit low thermal feedback at given dispersion of –3000 fs^2. An experimental evaluation of HD mirrors with substrates other than fused silica is in progress. Most importantly the pump power intensity of 8 kW/cm^2 was found to be limiting for this resonator configuration. Higher pump intensities up to

12 kW/cm^2 were also tried out but tended to impair KLM performance.

In summary, a simple geometric scaling procedure is proposed and implemented for increasing the peak and average power of Kerr-lens mode-locked thin-disk oscillators. Our experiments yield a linear increase in pulse energy with respect to the mode size in the Kerr medium. The presented concept holds promise for scaling femtosecond Kerr-lens mode-locked thin-disk oscillators toward pulse energies of hundreds of microjoules and average powers approaching the kilowatt frontier.

This work was supported by the Munich Centre for Advanced Photonics (MAP).

References

1. T. Eidam, S. Hanf, E. Seise, T. V. Andersen, T. Gabler, C. Wirth, T. Schreiber, J. Limpert, and A. Tünnermann, Opt. Lett. **35**, 94 (2010).
2. P. Russbueldt, T. Mans, J. Weitenberg, H. D. Hoffmann, and R. Poprawe, Opt. Lett. **35**, 4169 (2010).
3. J.-P. Negel, A. Voss, M. A. Ahmed, D. Bauer, D. Sutter, A. Killi, and T. Graf, Opt. Lett. **38**, 5442 (2013).
4. D. Bauer, I. Zawischa, D. H. Sutter, A. Killi, and T. Dekorsy, Opt. Express **20**, 9698 (2012).
5. C. J. Saraceno, F. Emaury, C. Schriber, M. Hoffmann, M. Golling, T. Südmeyer, and U. Keller, Opt. Lett. **39**, 9 (2014).
6. C. J. Saraceno, F. Emaury, O. H. Heckl, C. R. E. Baer, M. Hoffmann, C. Schriber, M. Golling, T. Südmeyer, and U. Keller, Opt. Express **20**, 23535 (2012).
7. S. V. Marchese, C. R. Baer, A. G. Engqvist, S. Hashimoto, D. J. Maas, M. Golling, T. Südmeyer, and U. Keller, Opt. Express **16**, 6397 (2008).
8. Y. Liu, S. Tschuch, M. Dürr, A. Rudenko, R. Moshammer, J. Ullrich, M. Siegel, and U. Morgner, Opt. Express **15**, 18103 (2007).
9. A. Giesen, H. Hügel, A. Voss, K. Wittig, U. Brauch, and H. Opower, Appl. Phys. B **58**, 365 (1994).
10. U. Keller, K. J. Weingarten, F. X. Kartner, D. Kopf, B. Braun, I. D. Jung, R. Fluck, C. Honninger, N. Matuschek, and J. Aus der Au, IEEE J. Sel. Top. Quant. Electron. **2**, 435 (1996).
11. F. X. Kärtner, *Few-Cycle Laser Pulse Generation and Its Applications*, 2004th ed., Vol. **95** of Topics in Applied Physics (Springer, 2004).
12. T. Brabec, P. F. Curley, C. Spielmann, E. Wintner, and A. J. Schmidt, J. Opt. Soc. Am. B **10**, 1029 (1993).
13. U. Morgner, F. X. Kärtner, S. H. Cho, Y. Chen, H. A. Haus, J. G. Fujimoto, E. P. Ippen, V. Scheuer, G. Angelow, and T. Tschudi, Opt. Lett. **24**, 411 (1999).
14. A. Stingl, R. Szipöcs, M. Lenzner, C. Spielmann, and F. Krausz, Opt. Lett. **20**, 602 (1995).
15. O. Pronin, J. Brons, C. Grasse, V. Pervak, G. Boehm, M.-C. Amann, V. L. Kalashnikov, A. Apolonski, and F. Krausz, Opt. Lett. **36**, 4746 (2011).
16. S. V. Marchese, T. Südmeyer, M. Golling, R. Grange, and U. Keller, Opt. Lett. **31**, 2728 (2006).
17. S. Naumov, A. Fernandez, R. Graf, P. Dombi, F. Krausz, and A. Apolonski, New J. Phys. **7**, 216 (2005).
18. L. Xu, G. Tempea, C. Spielmann, F. Krausz, A. Stingl, K. Ferencz, and S. Takano, Opt. Lett. **23**, 789 (1998).
19. C. Saraceno, C. Schriber, F. Emaury, O. Heckl, C. Baer, M. Hoffmann, K. Beil, C. Kränkel, M. Golling, T. Südmeyer, and U. Keller, Appl. Sci. **3**, 355 (2013).
20. A. Diebold, F. Emaury, C. Schriber, M. Golling, C. J. Saraceno, T. Südmeyer, and U. Keller, Opt. Lett. **38**, 3842 (2013).
21. K. Beil, C. J. Saraceno, C. Schriber, F. Emaury, O. H. Heckl, C. R. E. Baer, M. Golling, T. Südmeyer, U. Keller, C. Kränkel, and G. Huber, Appl. Phys. B **113**, 13 (2013).
22. J. Neuhaus, D. Bauer, J. Zhang, A. Killi, J. Kleinbauer, M. Kumkar, S. Weiler, M. Guina, D. H. Sutter, and T. Dekorsy, Opt. Express **16**, 20530 (2008).
23. G. Palmer, M. Schultze, M. Emons, A. L. Lindemann, M. Pospiech, D. Steingrube, M. Lederer, and U. Morgner, Opt. Express **18**, 19095 (2010).
24. A. A. Eilanlou, Y. Nabekawa, M. Kuwata-Gonokami, and K. Midorikawa, Jpn. J. Appl. Phys. **53**, 082701 (2014).
25. M. A. Larotonda, Opt. Commun. **228**, 381 (2003).
26. D. E. Spence, P. N. Kean, and W. Sibbett, Opt. Lett. **16**, 42 (1991).
27. F. Krausz, M. E. Fermann, T. Brabec, P. F. Curley, M. Hofer, M. H. Ober, C. Spielmann, E. Wintner, and A. J. Schmidt, IEEE J. Quantum Electron. **28**, 2097 (1992).
28. V. L. Kalashnikov, "Chirped-pulse oscillators: route to the energy-scalable femtosecond pulses," in *Solid State Laser*, A. Al-Khursan, ed. (InTech, 2012).
29. V. Magni, G. Cerullo, S. D. Silvestri, and A. Monguzzi, J. Opt. Soc. Am. B **12**, 476 (1995).
30. G. Cerullo, S. De Silvestri, V. Magni, and L. Pallaro, Opt. Lett. **19**, 807 (1994).
31. C. Spielmann, P. F. Curley, T. Brabec, and F. Krausz, IEEE J. Quantum Electron. **30**, 1100 (1994).
32. V. Magni, G. Cerullo, and S. De Silvestri, Opt. Commun. **101**, 365 (1993).
33. V. Pervak, O. Pronin, O. Razskazovskaya, J. Brons, I. B. Angelov, M. K. Trubetskov, A. V. Tikhonravov, and F. Krausz, Opt. Express **20**, 4503 (2012).
34. H. A. Haus, IEEE J. Sel. Top. Quant. Electron. **6**, 1173 (2000).
35. T. Brabec, C. Spielmann, and F. Krausz, Opt. Lett. **16**, 1961 (1991).
36. F. X. Kärtner, J. Aus der Au, and U. Keller, IEEE J. Sel. Top. Quant. Electron. **4**, 159 (1998).
37. V. L. Kalashnikov and A. Apolonski, Opt. Express **18**, 25757 (2010).
38. V. L. Kalashnikov, "Chirp-free solitons in dissipative systems: variational approximation and issue of the soliton energy scalability," http://info.tuwien.ac.at/kalashnikov/variational_soliton.pdf.
39. V. L. Kalashnikov is preparing a manuscript to be called "Energy scaling limits of Kerr-lens mode-locked oscillators."
40. R. Ell, U. Morgner, F. X. Kärtner, J. G. Fujimoto, E. P. Ippen, V. Scheuer, G. Angelow, T. Tschudi, M. J. Lederer, A. Boiko, and B. Luther-Davies, Opt. Lett. **26**, 373 (2001).
41. Y. Chen, F. X. Kärtner, U. Morgner, S. H. Cho, H. A. Haus, E. P. Ippen, and J. G. Fujimoto, J. Opt. Soc. Am. B **16**, 1999 (1999).
42. V. Magni, J. Opt. Soc. Am. A **4**, 1962 (1987).
43. W. Koechner, *Solid-State Laser Engineering*, 7th ed. (Springer, 2006).
44. H. Carstens, N. Lilienfein, S. Holzberger, C. Jocher, T. Eidam, J. Limpert, A. Tünnermann, J. Weitenberg, D. C. Yost, A. Alghamdi, Z. Alahmed, A. Azzeer, A. Apolonski, E. Fill, F. Krausz, and I. Pupeza, Opt. Lett. **39**, 2595 (2014).